

# Characterization of Structure and Properties of As-cast AlCuMg Alloys

Biljana Zlaticanin<sup>1</sup>, Branislav Radonjic<sup>1</sup> and Mirjana Filipovic<sup>2,\*</sup>

<sup>1</sup>The Faculty of Metallurgy and Technology, Cetinjski put bb, 81000 Podgorica, Serbia and Montenegro

<sup>2</sup>The Faculty of Technology and Metallurgy, Karnegijeva 4, 11000 Belgrade, Serbia and Montenegro

Early stages of transformation of a metastable AlCuMg alloy have been studied by DSC, X-ray powder diffraction method, quantitative microstructure analysis, hardness, compression strength and by scanning electron microscope. Differential scanning calorimetry has been done for samples: AlCu15Mg1 (0%Ti), AlCu15Mg1 (0.25%Ti), AlCu15Mg2 (0.25%Ti), AlCu15Mg3 (0%Ti), AlCu15Mg3 (0.25%Ti), AlCu15Mg4 (0.25%Ti), AlCu15Mg5 (0%Ti), AlCu15Mg5 (0.25%Ti). This method has produced DSC-curve, where endothermic effects are present, on the basis of which the heat of transition has been obtained. With increasing the magnesium and titanium content in the alloy, for the first and the second detectable endothermic effect, the value of heat of transition decreases. The formation of intermetallic compounds Al<sub>2</sub>Cu and Al<sub>2</sub>CuMg is monitored by X-ray powder diffraction. This method has shown that a tetragonal intermetallic compound Al<sub>2</sub>Cu and orthorhombic intermetallic compound Al<sub>2</sub>CuMg are formed for AlCuMg alloy. The effect of the magnesium and titanium content on the microstructure was monitored quantitatively. Using automatic image analysis we were able to measure the linear intercept grain size, the secondary dendrite arm spacing (DAS), the size of eutectic cells (Le), as well as the size distribution and volume fractions of the  $\alpha$ -solid solution and the eutectic. In alloys containing high magnesium the average values of the DAS and grain size were found to be reduced.

(Received July 2, 2003; Accepted December 2, 2003)

**Keywords:** aluminium-copper-magnesium alloy, as-cast structure, intermetallic compounds Al<sub>2</sub>Cu and Al<sub>2</sub>CuMg, lattice parameters, geometrical parameters, hardness and compression strength

## 1. Introduction

Excellent strength vs. density ratio, formability and corrosion resistance, make high-copper AlCuMg alloys a potential candidate for a number of industrial applications.<sup>1)</sup>

Developed in the early times in the aeronautical field, they have been then considered for a wide range of different applications, even though, due to their high specific strength, they are mainly considered as a substitute of iron-based materials for structural parts in the transportation industry. Several technical compositions are presently standardized and new alloys based on that metallic system are now being considered and developed.<sup>2)</sup>

A previous investigation<sup>3)</sup> tried to prove that alloys with higher content of copper (approximately 15 mass%) have tendency to nondendritic solidification. We have found it very interesting from both theoretical and practical point of view (semi-solid processing). We have also found that the most important parameters on forming and transformation of phases in these alloys are magnesium and titanium. In this investigation main attention was paid to mechanism of solidification and microstructure. The influence of chemical contents and structure on the mechanical properties (hardness and compression strength) was also investigated.

In these alloys aluminium is the primary constituent and in the cast alloys the basic structure consists of cored dendrites of aluminium solid solution, with a variety of constituents at the grain boundaries or interdendritic spaces, forming a brittle, more or less continuous network of eutectics. Copper has been the most common alloying element almost since the beginning of the aluminium industry, and a variety of alloys in which copper is the major addition were developed. Magnesium is usually combined with copper. The constituents formed in the alloys containing only one or more of copper, magnesium, etc. are soluble ones.

Depending on the alloy composition (say Cu content and Cu/Mg ratio), different phase distributions and consequently different material characteristics can be obtained. In this paper a DSC study of eight different AlCuMg alloys having a high copper content (15 mass%) and a Cu/Mg ratio 15; 7.5; 5; 3.75 and 3 respectively, is reported in order to investigate the effects of magnesium and titanium contents on the microstructure of AlCuMg alloys.

## 2. Experimental Procedure

Experimental work can be divided in two phases. The first phase comprises melting and casting of AlCuMg alloys. The solidification structure was modified by the addition of the AlTi5B1 to give alloys containing 0 to 0.25% titanium.

The second phase includes characterization of cast samples by differential scanning calorimetry, X-ray powder diffraction method, quantitative microstructure analysis and scanning electron microscope JCSA-733. The properties of these materials have been also examined including: hardness measuring and compression strength determining.

The composition of the alloys has been determined by wet analysis and the results are reported in Table 1.

DSC analyses have been performed in a differential scanning calorimeter type Shimadzu DSC-50 under protective argon atmosphere, at a scanning rate of 10°C/min, to the maximum temperature of 725°C. Mass of tested samples has been in range of 15.02–15.17 mg. Differential scanning calorimetry has been done for samples: AlCu15Mg1 (0%Ti), AlCu15Mg1 (0.25%Ti), AlCu15Mg2 (0.25%Ti), AlCu15Mg3 (0%Ti), AlCu15Mg3 (0.25%Ti), AlCu15Mg4 (0.25%Ti), AlCu15Mg5 (0%Ti), AlCu15Mg5 (0.25%Ti).

This method has produced DSC-curve on the basis of which next parameters have been calculated: heat of transition (Table 2 and Figs. 1–5). From the enclosed results of the testing it can be seen that addition of the titanium performs modification of the structure. If a result is a better

\*Corresponding author, E-mail: biljana@l.cis.cg.ac.yu

Table 1 Chemical composition of the investigated alloys (in mass%).

TYPE OF SAMPLE	%Al	%Fe	%Si	%Cu	%Zn	%Mg	%Ti	%V	%Cr
AlCu15Mg1 (0%Ti)	84.23	0.15	0.07	14.30	0.080	1.139	0.002	0.004	0.002
AlCu15Mg1 (0.25%Ti)	83.58	0.16	0.06	14.67	0.069	1.067	0.347	0.010	0.002
AlCu15Mg2 (0.25%Ti)	81.90	0.15	0.08	14.97	0.077	2.391	0.289	0.000	0.002
AlCu15Mg3 (0%Ti)	82.53	0.16	0.08	14.40	0.075	2.943	0.348	0.001	0.003
AlCu15Mg3 (0.25%Ti)	81.30	0.20	0.08	14.63	0.076	3.354	0.323	0.010	0.003
AlCu15Mg4 (0.25%Ti)	76.27	0.20	0.11	16.06	0.082	4.967	0.261	0.002	0.005
AlCu15Mg5 (0%Ti)	78.32	0.20	0.10	15.31	0.086	5.897	0.003	0.004	0.005
AlCu15Mg5 (0.25%Ti)	77.15	0.21	0.11	15.44	0.080	5.645	0.342	0.011	0.005

Table 2 Change of heat of transition of the investigated alloys with an increased titanium and magnesium content in the alloys.

TYPE OF SAMPLE	I PEAK			II PEAK			III PEAK		
	$T, ^\circ\text{C}$	$-\Delta H, \text{J/g}$	$-\Delta H, \text{J}$	$T, ^\circ\text{C}$	$-\Delta H, \text{J/g}$	$-\Delta H, \text{J}$	$T, ^\circ\text{C}$	$-\Delta H, \text{J/g}$	$-\Delta H, \text{J}$
AlCu15Mg1 (0%Ti)	504.9	1.83	0.029	537.6	27.67	0.45	615.2	68.35	1.12
AlCu15Mg1 (0.25%Ti)	506.3	3.87	0.054	537.6	32.90	0.46	608.9	54.39	0.76
AlCu15Mg2 (0.25%Ti)	512.4	45.98	0.67	—	—	—	602.5	52.75	0.77
AlCu15Mg3 (0%Ti)	515.2	49.70	0.74	—	—	—	599.3	53.73	0.88
AlCu15Mg3 (0.25%Ti)	514.0	53.04	0.82	—	—	—	595.8	51.75	0.72
AlCu15Mg4 (0.25%Ti)	—	—	—	522.2	72.07	0.78	581.6	33.53	0.36
AlCu15Mg5 (0%Ti)	—	—	—	523.1	59.74	0.99	596.0	44.06	0.73
AlCu15Mg5 (0.25%Ti)	—	—	—	526.9	75.75	1.24	578.7	28.28	0.46

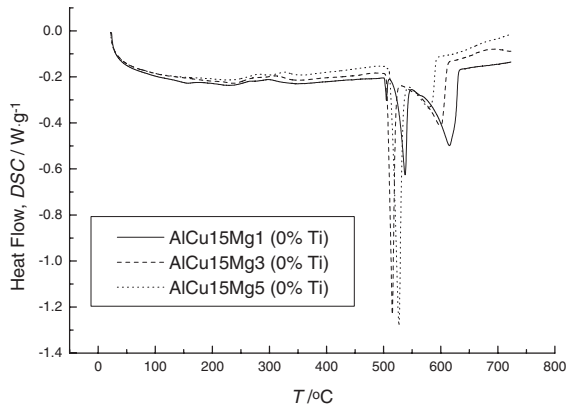


Fig. 1 DSC traces for alloys AlCu15Mg1 (0%Ti), AlCu15Mg3 (0%Ti) and AlCu15Mg5 (0%Ti) at 10°C/min.

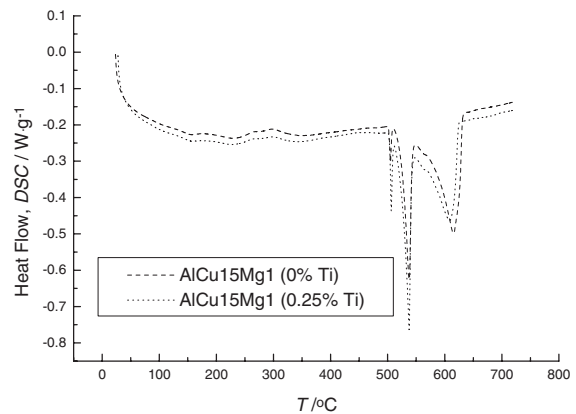


Fig. 3 DSC traces for alloys AlCu15Mg1 (0%Ti) and AlCu15Mg1 (0.25%Ti) at 10°C/min.

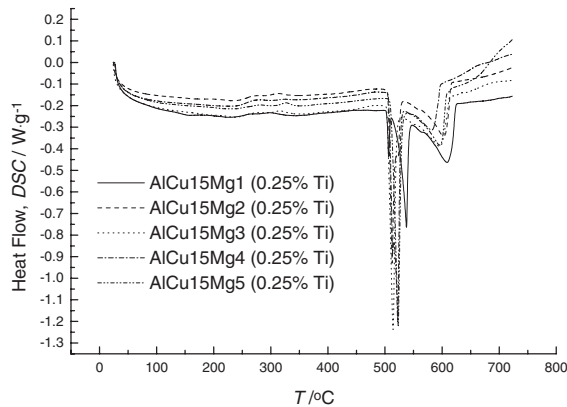


Fig. 2 DSC traces for alloys AlCu15Mg1 (0.25%Ti), AlCu15Mg2 (0.25%Ti), AlCu15Mg3 (0.25%Ti), AlCu15Mg4 (0.25%Ti) and AlCu15Mg5 (0.25%Ti) at 10°C/min.

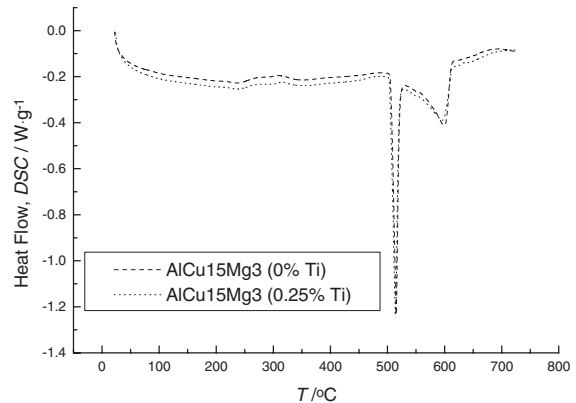


Fig. 4 DSC traces for alloys AlCu15Mg3 (0%Ti) and AlCu15Mg3 (0.25%Ti) at 10°C/min.

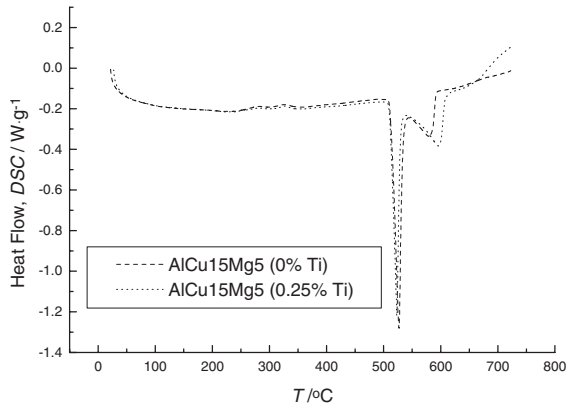


Fig. 5 DSC traces for alloys AlCu15Mg5 (0%Ti) and AlCu15Mg5 (0.25%Ti) at 10°C/min.

dispersion of insoluble components, porosity and nonmetal inclusions, it will improve mechanical properties.

The X-ray diffraction analysis was performed on the AlCu15Mg1 (0.25%Ti), AlCu15Mg2 (0.25%Ti), AlCu15Mg3 (0.25%Ti), AlCu15Mg4 (0.25%Ti) and AlCu15Mg5 (0.25%Ti) samples using a wide range of angles ( $2\theta$ ) from 5 to 100° with a step of 0.02° and a holding time of 0.50 seconds at each step. A diffractometer with a graphite monochromator and a constant divergence slit ( $D$ ) of 1 mm was used. The current and the voltage of the X-ray tube during the analysis were 30 mA and 40 kV, respectively. The width of the receiving slit ( $R$ ) was 0.1 mm, corresponding to fine focused X-ray tubes. The radiation was Cu  $K\alpha_1/\alpha_2$ , doublet ( $\lambda\alpha_1 = 0.154178$  nm and  $\lambda\alpha_2 = 0.154438$  nm).

The effect of the magnesium and titanium content on the microstructure was monitored quantitatively, using an automatic device for image analysis, QUANTIMET 500MC, and linear measuring method. Using automatic image analysis we were able to measure the grain size (minimum, maximum and average values-see Table 3), the dendrite arm spacing<sup>4</sup>-DAS (see Table 4), the eutectic cell length- $Le$  (see Table 5), the relative standard measuring errors ( $RSE$ ) for all the mention parameters, as well as the distribution by grain size and volume fractions of the  $\alpha$ -solid solution and the eutectic.

The Figs. 6–10 was obtained by applying scanning electron microscope JXA-733. The current and the voltage during the analysis for the copper, magnesium and titanium were  $1 \times 10^{-8}$  A and 20 kV, respectively, and we applied  $K\alpha$  radiation.

Hardness has been measured by use of the Brinell method. Compression strength of the samples of cast alloys has been

Table 3 Grain size for different titanium contents in investigated alloys.

Type of sample	Average, $\mu\text{m}$	min, $\mu\text{m}$	max, $\mu\text{m}$	$RSE$ , %
AlCu15Mg1 (0%Ti)	233.37	45	525	3.98334
AlCu15Mg1 (0.25%Ti)	74.62	30	165	3.44239
AlCu15Mg2 (0.25%Ti)	72.44	30	155	3.88769
AlCu15Mg3 (0%Ti)	204.00	45	600	2.98336
AlCu15Mg3 (0.25%Ti)	70.44	30	180	2.33245
AlCu15Mg4 (0.25%Ti)	52.88	15	150	3.22437
AlCu15Mg5 (0%Ti)	99.13	30	180	2.88654
AlCu15Mg5 (0.25%Ti)	48.46	15	90	2.66438

Table 4 Dendrite arm spacing (DAS) for different titanium contents in the investigated alloys.

Type of sample	average, $\mu\text{m}$	min, $\mu\text{m}$	max, $\mu\text{m}$	$RSE$ , %	$V_v$ , <i>ah.s.</i> vol%
AlCu15Mg1 (0%Ti)	20.92	0.83	102	2.44727	73.401
AlCu15Mg1 (0.25%Ti)	15.92	0.83	107	1.99096	73.033
AlCu15Mg2 (0.25%Ti)	15.83	0.83	106	1.89952	68.273
AlCu15Mg3 (0%Ti)	15.53	0.83	121	1.80886	66.882
AlCu15Mg3 (0.25%Ti)	14.45	0.83	89	1.85417	66.742
AlCu15Mg4 (0.25%Ti)	14.06	0.83	90	1.77149	54.662
AlCu15Mg5 (0%Ti)	15.05	0.83	90	1.77178	54.234
AlCu15Mg5 (0.25%Ti)	14.05	0.83	108	2.01943	51.437

Table 5 The linear intercept size of eutectic cells ( $Le$ ) for different titanium contents in the investigated alloys.

Type of sample	average, $\mu\text{m}$	min, $\mu\text{m}$	max, $\mu\text{m}$	$RSE$ , %	$V_v$ , <i>e.</i> vol%
AlCu15Mg1 (0%Ti)	4.28	0.32	50.00	2.29782	26.463
AlCu15Mg1 (0.25%Ti)	3.62	0.32	41.29	2.07753	26.668
AlCu15Mg2 (0.25%Ti)	4.57	0.32	52.26	2.27030	31.324
AlCu15Mg3 (0%Ti)	5.84	0.32	71.61	2.59711	33.059
AlCu15Mg3 (0.25%Ti)	5.73	0.32	52.58	2.58284	33.128
AlCu15Mg4 (0.25%Ti)	9.37	0.32	111.94	2.73655	45.150
AlCu15Mg5 (0%Ti)	9.53	0.32	72.20	2.73457	45.595
AlCu15Mg5 (0.25%Ti)	9.41	0.32	101.94	2.59173	48.225

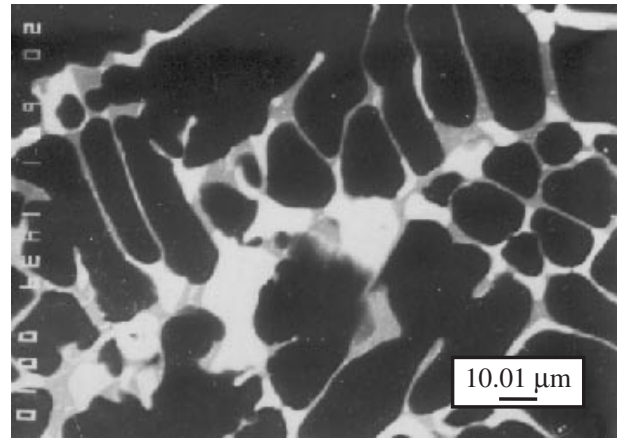


Fig. 6 Microstructure of alloy AlCu15Mg1 (0.25%Ti),  $\times 600$ .

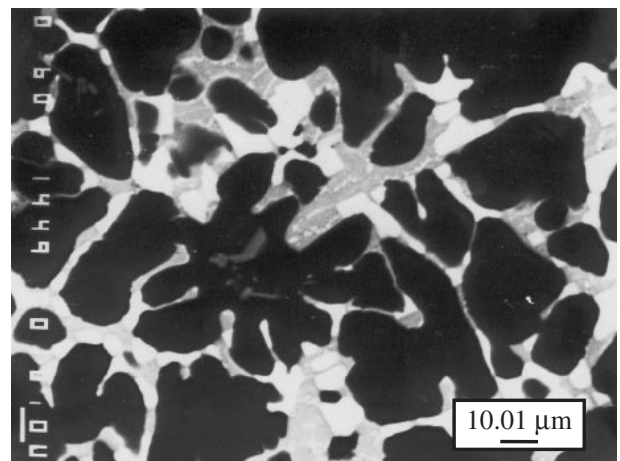


Fig. 7 Microstructure of alloy AlCu15Mg2 (0.25%Ti),  $\times 600$ .

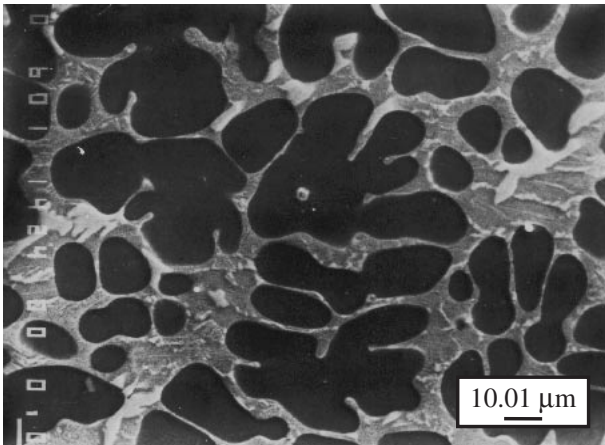


Fig. 8 Microstructure of alloy AlCu15Mg3 (0.25%Ti),  $\times 600$ .

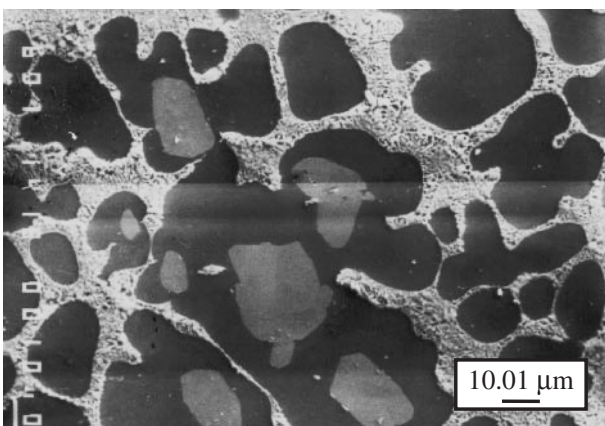


Fig. 9 Microstructure of alloy AlCu15Mg4 (0.25%Ti),  $\times 600$ .

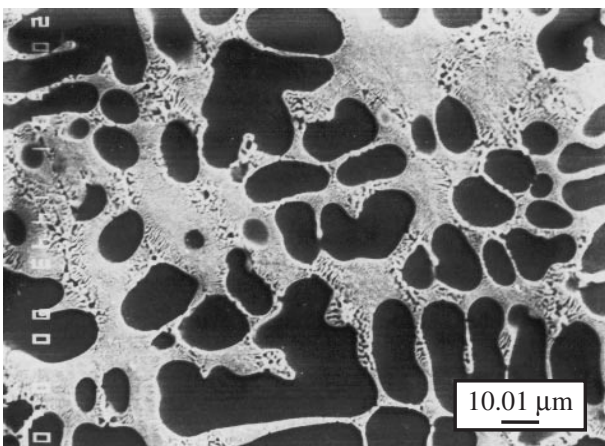


Fig. 10 Microstructure of alloy AlCu15Mg5 (0.25%Ti),  $\times 600$ .

tested on a universal electronic tensile testing machine of  $1 \times 10^4$  kg. Average size of samples was as follows: diameter  $D_0 = 10$  mm and height  $H_0 = 20$  mm. All of the tested samples have been fractured. Compression strength is measured in the moment of fracture. The Yield strength is estimated by graphical analysis.

### 3. Results and Discussion

#### 3.1 Differential scanning calorimetry analysis

DSC traces obtained at  $10^\circ\text{C}/\text{min}$  from the investigated

alloys are shown in Figs. 1–5. Thermograms obtained for high-copper AlCuMg alloys (Figs. 1–5) can be briefly described as follows: a) a “low temperature” section ranging between room temperature and  $500^\circ\text{C}$  where several endo- and exothermal effects are present; b) an “intermediate temperature” section between  $500^\circ\text{C}$  and  $550^\circ\text{C}$ , where only endothermal effects can be detected, c) a “high temperature” section between  $550^\circ\text{C}$  and  $700^\circ\text{C}$  where a broad endothermic effect is present.

In the thermograms reported in Figs. 1–5, where three endothermal effects are present for the alloy AlCu15Mg1 and two endothermal effects are present for the alloys AlCu15Mg2, AlCu15Mg3, AlCu15Mg4, AlCu15Mg5, the first detectable thermal effect is the intermediate temperature endothermal peak. It refers to a phase transition with the reaction enthalpy of  $-1.83$  J/g for alloy AlCu15Mg1 (0%Ti) and  $-3.87$  J/g for alloy AlCu15Mg1 (0.25%Ti). Temperature of the first peak is  $505^\circ\text{C}$  for alloy AlCu15Mg1 (0%Ti). These results show that the first peak is due to the localized melting with the formation of a melt rich in copper and magnesium in the presence of the  $\alpha$  solid solution and the compounds  $\text{Al}_2\text{Cu}$  and  $\text{Al}_2\text{CuMg}$ . In alloys in which the copper: magnesium ratio is more than 8:1 the main hardening phase is  $\text{Al}_2\text{Cu}$  ( $\theta$ ); in the alloys in the range 8:1 to 4:1 the main hardening phases are  $\text{Al}_2\text{Cu}$  and  $\text{Al}_2\text{CuMg}$ . Between 4:1 and 1.5:1 the main hardening phase is  $\text{Al}_2\text{CuMg}$ . Also, these results show that with the increased titanium content in the alloy, value of the heat of transition is decreased from  $-1.83$  J/g for alloy AlCu15Mg1 (0%Ti) to  $-3.87$  J/g for alloy AlCu15Mg1 (0.25%Ti) (see Table 2). Also, it is possible to see that with the increased magnesium content in the alloy, the value of the heat of transition is decreased from  $-1.83$  J/g for alloy AlCu15Mg1 (0%Ti) to  $-49.70$  J/g for alloy AlCu15Mg3 (0%Ti) (see Table 2).

In the thermograms reported in Figs. 1–5 the second detectable thermal effect is the intermediate temperature endothermal peak. It refers to a phase whose activation energy is  $-27.67$  J/g for alloy AlCu15Mg1 (0%Ti) and  $-32.90$  J/g for alloy AlCu15Mg1 (0.25%Ti). From these results and results of the X-ray analysis of samples after heating on  $540^\circ\text{C}$  it is possible to conclude that for this alloys the second peak can be assigned to the local melting of the ternary eutectic. Also, these results prove that with the increased titanium content in the alloy, value of the heat of transition is decreased (see Table 2). Also, it is seen that with the increased magnesium content in the alloy, value of the heat of transition is decreased from  $-32.90$  J/g for alloy AlCu15Mg1 (0.25%Ti) over  $-72.07$  J/g for alloy AlCu15Mg4 (0.25%Ti) to  $-75.75$  J/g for alloy AlCu15Mg5 (0.25%Ti) (see Table 2).

In the thermograms reported in Figs. 1–5 the third detectable thermal effect is the high temperature endothermal peak. It refers to a phase whose activation energy is  $-68.35$  J/g for alloy AlCu15Mg1 (0%Ti) and  $-54.39$  J/g for alloy AlCu15Mg1 (0.25%Ti); or  $-44.06$  J/g for alloy AlCu15Mg5 (0%Ti) and  $-28.28$  J/g for alloy AlCu15Mg5 (0.25%Ti). On the basis of these results it is possible to conclude that for these alloys the third peak shows thermal events associated with localized melting of the binary eutectic. It is seen that with the increased magnesium content

in the alloy, value of the heat of transition is increased from  $-68.35 \text{ J/g}$  for alloy AlCu15Mg1 (0%Ti) over  $-53.73 \text{ J/g}$  for alloy AlCu15Mg3 (0%Ti) to  $-44.06 \text{ J/g}$  for alloy AlCu15Mg5 (0%Ti) (see Table 2). Also, the results show that with the increased titanium content in the alloy, value of the heat of transition is increased from  $-68.35 \text{ J/g}$  for alloy AlCu15Mg1 (0%Ti) to  $-54.39 \text{ J/g}$  for alloy AlCu15Mg1 (0.25%Ti) (see Table 2). With the increased titanium content in the alloy, value of the temperature of the third peak is decreased on example from  $615.17^\circ\text{C}$  for alloy AlCu15Mg1 (0%Ti) to  $608.97^\circ\text{C}$  for alloy AlCu15Mg1 (0.25%Ti) (see Table 2). Also with the increased magnesium content in the alloy, value of the temperature of the third peak is decreased, for example, from  $615.2^\circ\text{C}$  for alloy AlCu15Mg1 (0%Ti) to  $596.0^\circ\text{C}$  for alloy AlCu15Mg5 (0%Ti) (see Table 2).

### 3.2 Quantitative microstructure analysis

In this paper, the effects of magnesium and titanium contents on the microstructure and properties of AlCuMg alloy were examined. The as-cast structure was modified by the addition of the AlTi5B1 to give alloys containing 0 to 0.25 mass% titanium. Namely, copper content in the standard alloys ranges up to around 5% since the maximum solubility of copper in eutectic temperature ( $548^\circ\text{C}$ ) is 5.65%. Standard industrial aluminium-copper alloys solidify with the formation of a dendritic structure, however, a tendency to form with a globular structure at higher copper contents was reported<sup>5,6</sup> and eutectic appears in the interdendritic space and between grains.

In the binary aluminium-copper system, the aluminium-rich terminal solid solution is in equilibrium with the intermetallic compound  $\theta$ , which has approximately the formula  $\text{CuAl}_2$ , although some solid solubility exists. The addition of magnesium allows the formation of more intermetallic compounds, such as  $\text{CuMgAl}_2$ ,  $\text{CuMg}_4\text{Al}_6$ ,  $\text{CuMgAl}$  and  $\text{Cu}_6\text{Mg}_2\text{Al}_5$ , as illustrated in Fig. 11 by the isothermal section at  $430^\circ\text{C}$  for the ternary system. Magnesium increases<sup>5</sup> the strength and hardness of the alloys, but, especially in castings, this is accompanied by a decrease in ductility and impact resistance. Titanium is added as grain refiner and it is very effective in reducing the grain size. Grain size controls the distribution<sup>6</sup> of porosity and constituents, and for this reason the properties of the high-copper alloys are very sensitive to grain size.

These investigated AlCuMg alloys without titanium have typical dendritic structures. Micrographs show dendrites of aluminium solid solution as the primary phase, with a eutectic mixture filling the interdendritic spaces. The eutectic is of the divorced type-particles of a second phase in a solid solution. The second phase can be an intermetallic compounds that contain aluminium and one or more alloying elements ( $\text{Al}_2\text{Cu}$  and  $\text{Al}_2\text{CuMg}$ ); intermetallic compounds that do not necessarily contain aluminium ( $\text{Mg}_2\text{Cu}$  or  $\text{MgCu}_2$ ); or an alloying element, such as copper or magnesium, without depending on the composition of the alloy. Investigated AlCuMg alloys with titanium have typical cellular structures. Cast AlCuMg alloys contain soluble phases:  $\text{Al}_2\text{Cu}$  or  $\text{Al}_2\text{CuMg}$  which appear in various amounts and at various locations in the microstructure, depending on the thermal history of the specimen.

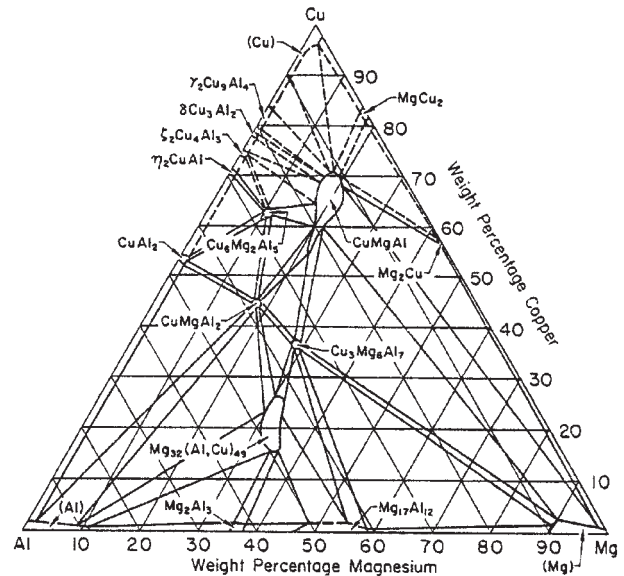


Fig. 11 Isothermal section at  $430^\circ\text{C}$  for the Al-Cu-Mg system. (Adapted from Metals Handbook, 8th Ed., Vol 8, American Society for Metals, Metals Park, Ohio, 1973).

The Figs. 6–10 were obtained by applying scanning electron microscope JCSA-733. There is copper and a little magnesium in the white phase. X-ray analysis confirmed that the gray phase of eutectic contains magnesium, but copper exist in lighter phases. Titanium is obtained in the form of little plates in some areas of eutectic but only in the white phase. It also exists inside the grain.

Using automatic image analysis we were able to measure the grain size (minimum, maximum and average values), dendrite arm spacing-DAS, the eutectic cell length- $Le$ , the relative standard measuring errors-RSE and volume fractions of the  $\alpha$ -solid solution and the eutectic.

Measurement of dendrite arm spacing is accomplished in the same manner as grain size measurement, that is, by the intercept method. Dendrite arm spacing is an important consideration in cast aluminium-copper-magnesium alloy microstructures. From the results of these measurements, it is possible to obtain information on the rate of solidification of the material and therefore on some indication of the strength of the material. For example, the finer the dendrite arm spacing is, the higher the strength.

Measured grain sizes are expressed in the mean diameter per grain. Grain size and structure of dendrite and eutecticum depend on processing parameters,<sup>7</sup> first of all on melt temperature and the solidification rate. Material properties also depend on the last two items. Also, addition of a grain refiner (AlTi5B1) resulted in the nearly equiaxed structure shown in micrographs. The addition of titanium and boron in form of the alloy AlTi5B1 are used to produce particles of  $\text{TiB}_2$  in the melt. These particles are then the nuclei for the  $\text{TiAl}_3$  phase that affects the solidification. Titanium and aluminium produce a peritectic reaction with the  $\text{TiAl}_3$  and the solid peritectic acts as a solidification nucleus for pure aluminium and its solid solutions. The reduction in grain size and dendrite arm spacing, and also improvement in structure uniformity as a result of adding a grain refiner is shown in Figs. 6–10 and Table 3–4. Also, size and shape are affected

by the addition of magnesium. With increased amounts of magnesium for the same content of titanium in the alloy, the average values of the dendrite arm spacing and grain size are decreased, and we obtain a fine, uniform grain structure, as shown in micrographs and Table 3–4. Also, in alloys containing high magnesium the average values of the eutectic cell length and volume fractions of the eutectic were found to increase (Table 5). Chemical composition affects structure through its influence on phase relations.

### 3.3 Results of the X-ray analysis

Using X-ray powder diffraction we concluded that for AlCuMg alloys the tetragonal intermetallic compound  $Al_2Cu$  and orthorhombic intermetallic compound  $Al_2CuMg$  are formed across the whole range of magnesium addition. Obtained results for the lattice parameters of tetragonal intermetallic compound  $Al_2Cu$  are: for AlCu15Mg1 alloy  $a = 0.6087$  nm,  $c = 0.4858$  nm and  $V = 0.180$  nm<sup>3</sup>; for AlCu15Mg2 alloy  $a = 0.6074$  nm,  $c = 0.4870$  nm and  $V = 0.1797$  nm<sup>3</sup>; for AlCu15Mg3 alloy  $a = 0.6067$  nm,  $c = 0.4831$  nm and  $V = 0.1778$  nm<sup>3</sup>; for AlCu15Mg4 alloy  $a = 0.6071$  nm,  $c = 0.4862$  nm and  $V = 0.1792$  nm<sup>3</sup>; for AlCu15Mg5 alloy  $a = 0.6065$  nm,  $c = 0.4767$  nm and  $V = 0.1754$  nm<sup>3</sup>. Obtained results for the lattice parameters of orthorhombic intermetallic compound  $Al_2CuMg$  are: for AlCu15Mg1 alloy  $a = 0.4023$  nm,  $b = 0.9209$  nm,  $c = 0.7138$  nm and  $V = 0.2644$  nm<sup>3</sup>; for AlCu15Mg2 alloy  $a = 0.4016$  nm,  $b = 0.9218$  nm,  $c = 0.7142$  nm and  $V = 0.2644$  nm<sup>3</sup>; for AlCu15Mg3 alloy  $a = 0.4014$  nm,  $b = 0.9208$  nm,  $c = 0.7135$  nm and  $V = 0.2637$  nm<sup>3</sup>; for AlCu15Mg4 alloy  $a = 0.4000$  nm,  $b = 0.9250$  nm,  $c = 0.7150$  nm and  $V = 0.2646$  nm<sup>3</sup>; for AlCu15Mg5 alloy  $a = 0.4008$  nm,  $b = 0.9246$  nm,  $c = 0.7173$  nm and  $V = 0.2658$  nm<sup>3</sup>. Obtained results for the lattice parameters of the intermetallic compounds are in compliance with the published data from literature: JCPDS card 25 0012 for  $Al_2Cu$  are  $a = 0.6065$  nm,  $c = 0.4873$  nm and  $V = 0.1792$  nm<sup>3</sup>; and JCPDS card 28 0014 for  $Al_2CuMg$  are  $a = 0.4000$  nm,  $b = 0.9250$  nm,  $c = 0.7150$  nm and  $V = 0.2646$  nm<sup>3</sup>. Also, from the X-ray diffractograms the microstructural parameter have been calculated: the average sub-grain size (Table 6).

The sub-grain is the range of the lattice of the crystal grain from which the X-rays are coherently diffracted. The sub-grains are separated by dislocation walls and have a space orientation which is different by several angle minutes. Using X-ray diffraction of polycrystals, the sub-grain is defined as a range of quantitative values, starting from the average length in a definite crystallographic direction, through the average volume, to their dimensional distributions. In alloys contain-

Table 7 Hardness and compression strength of the investigated alloys with different amounts titanium and magnesium.

Type of sample	HB average	$R_{p0.2}$ (MPa)	$R_m$ (MPa)
AlCu15Mg1 (0%Ti)	146	264.86	673.67
AlCu15Mg1 (0.25%Ti)	148	274.63	674.88
AlCu15Mg2 (0.25%Ti)	153	283.34	678.92
AlCu15Mg3 (0%Ti)	155	302.20	680.08
AlCu15Mg3 (0.25%Ti)	159	334.16	689.17
AlCu15Mg4 (0.25%Ti)	160	369.19	698.66
AlCu15Mg5 (0%Ti)	161	372.78	705.46
AlCu15Mg5 (0.25%Ti)	167	379.88	712.25

ing high magnesium the average sub-grain size in the crystallographic direction [112] were found to increase.

### 3.4 Mechanical properties

The Brinell hardness and the compression strength are shown in Table 7. The changes in chemical composition of the alloy cause changes in the structure and these changes are reflected in the Brinell hardness and the compression strength. The hardness of the modified alloy is higher than the hardness of the alloy without any modification treatment. By increasing the content of magnesium and titanium the hardness and compression strength also increase.

## 4. Conclusions

Different parameters obtained as a result a application various analysis on the aluminium-copper-magnesium alloys enable us to explain influence of magnesium and titanium contents on the mode of formation and the structure in that system. From the obtained data the following conclusions can be drawn:

— For AlCuMg alloys the first peak from thermograms reported in Figs. 1–5 can be assigned to the localized melting with the formation of a melt rich in copper and magnesium in presence of the  $\alpha$  solid solution and the compounds  $Al_2Cu$  and  $Al_2CuMg$ .

— With the increased magnesium and titanium content in the alloy for the first and for the second peak from thermograms, value of the heat of transition is decreased, but for third peak with the increased content of magnesium and titanium value of the heat of transition is increased (see Table 2 and Fig. 1–5).

— For these alloys the second peak from thermograms can be assigned to the local melting of the ternary eutectic and the third peak showing thermal events is associated with local melting of the binary eutectic.

— With the increased amounts of magnesium for the same content of titanium in the alloy, the average values of the dendrite arm spacing and grain size are decreased (see Tables 3 and 4).

— With the same chemical composition of AlCuMg alloy but increased titanium content, the average value of the grain size is decreased (see Table 3). Besides, the presence of titanium causes a decrease in the medium value of the dendrite arm spacing ( $DAS$ ) and length eutectic ( $Le$ ) (see Tables 4 and 5). With the addition of AlTi5B1, a modification to the solidification structure and smaller solidification grains are

Table 6 Average sub-grain size in the crystallographic direction [112] for different magnesium contents in aluminium-copper-magnesium alloys.

Type of sample	Average sub-grain size, nm
AlCu15Mg1 (0.25%Ti)	19.3
AlCu15Mg2 (0.25%Ti)	38.6
AlCu15Mg3 (0.25%Ti)	43.6
AlCu15Mg4 (0.25%Ti)	48.6
AlCu15Mg5 (0.25%Ti)	49.1

obtained. We confirmed that titanium is a very effective grain refiner. The resulting dispersion of insoluble components as well as a smaller porosity and fewer non-metal inclusions improved the mechanical properties.

— Across the whole range of magnesium content tested has been found out that for AlCu15MgX alloys a tetragonal intermetallic compound Al<sub>2</sub>Cu and orthorhombic intermetallic compound Al<sub>2</sub>CuMg are formed.

— Compression strength and hardness of the aluminium-copper-magnesium alloys increase with the content of titanium and magnesium (Table 7).

## REFERENCES

- 1) I. J. Polmear: *Light Alloys*, (Arnold, London 1995) pp. 124–127.
- 2) P. Ratchev, B. Verlinden, P. De Smet and P. Van Houtte: *Mater. Trans., JIM* **40** (1999) 34–43.
- 3) B. Zlaticanin: *The effects of titanium and boron contents in the aluminium-copper alloys on dependence in the triad technology-structure-properties*, (Masters thesis, Belgrade 1999), pp. 20–67.
- 4) AM. Samuel and FH. Samuel: *J. of Mater. Sci.* **30** (1995) 1698–1708.
- 5) L. F. Mondolfo: *Aluminium Alloys: Structure and Properties*, (Butterworth and Co (Publishers) Ltd, London 1976) pp. 245–266.
- 6) X. Yang, J. D. Hunt and D. V. Edmonds: *Aluminium, Jahrgang* **69** (1993) 158–162.
- 7) B. Radonjic: *Aluminium, Jahrgang* **58** (1982) 646–649.